NEW YORK UNIVERSITY
INSTITUTE OF MATHEMATICAL SCIENCES
LIBRARY
25 Waverly Place, New York 3, N. Y.

LOF

AEC Computing and Applied Mathematics Center

NOV 7

AEC RESEARCH AND DEVELOPMENT REPORT

PHYSICS NYO-7978

NON-LINEAR BENDING AND BUCKLING OF CIRCULAR PLATES

by

Herbert B. Keller and Edward L. Reiss

February 1, 1958

Institute of Mathematical Sciences

NEW YORK UNIVERSITY
NEW YORK, NEW YORK

c. 1

This report was prepared as an account of Government sponsored work. Neither the United States, nor the Commission, nor any person acting on behalf of the Commission:

A. Makes any warranty or representation, express or implied, with respect to the accuracy, completeness, or usefulness of the information contained in this report, or that the use of any information, apparatus, method, or process disclosed in this report may not infringe privately owned rights; or

B. Assumes any liabilities with respect to the use of, or for damages resulting from the use of any information, apparatus, method, or process disclosed in this report.

As used in the above, "person acting on behalf of the Commission" includes any employee or contractor of the Commission to the extent that such employee or contractor prepares, handles or distributes, or provides access to, any information pursuant to his employment or contract with the Commission.

AEC Computing and Applied Mathematics Center
Institute of Mathematical Sciences
New York University

PHYSICS NYO-7978

NON-LINEAR BENDING AND BUCKLING OF CIRCULAR PLATES

by

Herbert B. Keller and Edward L. Reiss

February 1, 1958

Contract No. AT(30-1)-1480

NYO-7978
PHYSICS AND
MATHEMATICS

ABSTRACT

An iterative method for solving certain boundary value problems that occur in a non-linear theory of thin elastic plates and shells has been developed [10] and applied to obtain numerical solutions of the von Kármán plate equations for a variety of bending and buckling problems. In this report, the method and solutions are presented for circular plates subjected to either uniform lateral pressure or uniform edge thrust and with various edge conditions.

The solutions yield a complete description of stresses and deflections for an apparently unlimited range of load parameters. Boundary layer phenomena are clearly observed and are discussed. The iterative method proves to be superior to the previously used power series method and it is applicable to other non-linear problems.

NON-LINEAR BENDING AND BUCKLING OF CIRCULAR PLATES

TABLE OF CONTENTS

Page

Abstract.... 2
I. Introduction.... 4
II. Mathematical Formulation.... 6
III. Numerical Formulation and Iterative Solutions.... 9
IV. Computational Procedures.... 14
V. Discussion of Results.... 17
Bibliography.... 22
Appendix: Theoretical Convergence Properties.... 24

NON-LINEAR BENDING AND BUCKLING OF CIRCULAR PLATES

1. Introduction.

In this paper we consider a thin circular elastic plate of thickness t and radius R subjected either to a uniform lateral pressure, p, or to a uniform edge thrust, f. The first loading situation is referred to as a bending problem and the second as a buckling problem. In both cases only rotationally symmetric deformations will be considered so that all deflections and stresses are functions of a single radial coordinate, r.

It is well known that the classical linear theory of plates yields solutions of these problems which are valid only for a limited range of low loads. For larger values of p and f it is necessary to apply non-linear plate theories which allow for finite deflections and account for the interaction of membrane and bending stresses. Thus we employ the von Kármán equations [1] which are based on a non-linear theory of elasticity with infinitesimal strains and are valid for flat plates undergoing small but finite displacements. For rotationally symmetric deformations of circular plates these equations reduce to two coupled second order non-linear ordinary differential equations.

The first extensive investigation of the bending problem for a clamped plate was given by Way [2]. He employed power series to tabulate solutions of the von Kármán equations for pressures just into the non-linear range. Subsequently, Friedrichs and Stoker [3,4] gave a complete treatment of the buckling problem for simply supported plates. They obtained solutions by means of perturbations, power series and asymptotic expansions for respectively, small, intermediate and large values of the edge thrust. In addition a boundary layer effect was discovered in which rapid changes of stress become concentrated in a narrow band at the edge of the plate as f increases. These methods were applied by Bromberg [5] to the bending problem for three different edge conditions. The boundary layer was again studied in detail and shown to be somewhat more complicated than in the buckling case. Other treatments, using the above-mentioned techniques, have been given by Chien [6,7] and Bodner [8] for bending and buckling problems respectively. In all of these studies power series solutions could be obtained only for limited values of load. Green and Southwell [9] applied relaxation techniques to finite difference approximations of a bending and a buckling problem for comparatively low loads. However the convergence of their procedure has not been studied and it is not convenient for application to a large range of load parameters. In addition, a special Rayleigh-Ritz procedure was required in treating the buckling problem.

In this paper we present a numerical method for solving non-linear bending and buckling problems of circular plates.

The method consists of approximating the von Kármán equations by corresponding finite difference equations and then solving this non-linear algebraic system by an "interpolated" iterative procedure. A theoretical study of the convergence of this procedure has been given [10] and some of these results are summarized in the Appendix. This study and numerous applications of the method indicate that it yields accurate solutions for an unlimited range of loads. Thus a more extensive study of the development of boundary layer phenomena is possible. Furthermore, the method is applicable in its present form to other one dimensional non-linear elasticity problems. With proper modifications, it may be applicable to two dimensional bending and buckling problems.

2. Mathematical Formulation.

Let $w(r)$ be the deflection of the plate normal to the unstrained middle surface, $\Phi(r)$ be the Airy Stress Function and p be the uniform lateral pressure. Then in terms of the dimensionless variables

$$x \equiv \frac{r}{R} \quad , \quad \gamma(x) \equiv \frac{-[12(1-\nu^2)]}{ER} \left(\frac{R}{t}\right)^2 \frac{d\Phi(r)}{dr} \quad ,$$

(1)

$$\alpha(x) \equiv -[12(1-\nu^2)]^{1/2}\left(\frac{R}{t}\right) \frac{dw(r)}{dr} \quad , \quad P \equiv \frac{[12(1-\nu^2)]^{3/2}}{2E} \left(\frac{R}{t}\right)^4 p,$$

the von Kármán equations [1], in polar coordinates for rotationally symmetric deformations, reduce to

(2a) $$L\,\alpha(x) = -\,\alpha(x)\,\gamma(x) - Px^2 \quad ,$$

(2b) $$L\,\gamma(x) = \frac{1}{2}\,\alpha^2(x) \quad .$$

Here we have introduced the linear differential operator

$$L \equiv x\,\frac{d}{dx}\,\frac{1}{x}\,\frac{d}{dx}\,x \quad ,$$

and in (1) E is Young's Modulus and ν is Poisson's ratio.

The radial and circumferential membrane stresses, σ_R and σ_C respectively, and the corresponding reduced stresses $\sum_R$ and $\sum_C$, are given in terms of the new stress function, $\gamma(x)$, by

(3a) $$\textstyle\sum_R(x) \equiv \frac{12(1-\nu^2)}{E}\left(\frac{R}{t}\right)^2 \sigma_R(r) = -\,\frac{\gamma(x)}{x} \quad ,$$

(3b) $$\textstyle\sum_C(x) \equiv \frac{12(1-\nu^2)}{E}\left(\frac{R}{t}\right)^2 \sigma_C(r) = -\,\frac{d\gamma(x)}{dx} \quad .$$

The radial and circumferential bending stresses, σ_R^B and σ_C^B respectively, and the corresponding reduced stresses $\sum_R^B$ and $\sum_C^B$ are given in terms of the negative slope, $\alpha(x)$, by

(3c) $$\textstyle\sum_R^B(x) \equiv \frac{[12(1-\nu^2)]^{3/2}}{6E}\left(\frac{R}{t}\right) \sigma_R^B(r) = \frac{d\alpha(x)}{dx} + \nu\,\frac{\alpha(x)}{x} \quad ,$$

(3d) $$\textstyle\sum_C^B(x) \equiv \frac{[12(1-\nu^2)]^{3/2}}{6E}\left(\frac{R}{t}\right)^2 \sigma_C^B(r) = \nu\,\frac{d\alpha(x)}{dx} + \frac{\alpha(x)}{x} \quad .$$

Boundary conditions at the center, $x = 0$, and edge of the plate, $x = 1$, must be specified to complete the formulation. From the assumed symmetry and regularity at the center it is necessary that

$$(4) \qquad \alpha(0) = \gamma(0) = 0 \ .$$

At the edge, conditions of the following form are considered,

$$(5) \qquad a\,\frac{d\alpha(1)}{dx} + b\alpha(1) = 0, \quad c\,\frac{d\gamma(1)}{dx} + d\gamma(1) = F \ .$$

Here a, b, c and d are constants which define a particular problem, and $F = -\frac{12(1-\nu^2)}{E}\left(\frac{R}{t}\right)^2 f$ is the dimensionless edge thrust. We consider in this paper five special cases of (5):

A) Clamped and radial displacement equal to zero,
$a = 0,\ b = 1,\ c = 1,\ d = -\nu,\ F = 0.$

B) Simply supported and radial displacement equal to zero,
$a = 1,\ b = \nu,\ c = 1,\ d = -\nu,\ F = 0.$

C) Simply supported and radial membrane stress equal to zero,
$a = 1,\ b = \nu,\ c = 0,\ d = 1,\ F = 0.$

D) Simply supported and radial membrane stress specified,
$a = 1,\ b = \nu,\ c = 0,\ d = 1,\ F \geq 0.$

E) Clamped and radial membrane stress specified,
$a = 0,\ b = 1,\ c = 0,\ d = 1,\ F \geq 0.$

Problems A, B and C are bending problems $(P \neq 0)$

and have been discussed in a previous paper [5]. Problems D and E are buckling problems for which $P = 0$. D is the case considered by Friedrichs and Stoker [3,4] and E by Bodner [8].

Equations (2), (4) and (5) form a complete statement of the problems to be solved. We seek solutions for a wide range of the loading parameters P and F.

3. Numerical Formulation and Iterative Solutions.

To obtain numerical solutions we proceed by placing a uniform mesh of points

$$(6) \qquad x_i = i\delta x \quad , \quad \delta x = \frac{1}{m} \quad , \quad i = 0, 1, \ldots, m \quad ,$$

on the dimensionless radius of the plate, $0 \leq x \leq 1$. The functions $\alpha(x)$ and $\gamma(x)$ are then approximated by "mesh functions" $\overline{\alpha}(x_i)$ and $\overline{\gamma}(x_i)$ which are defined only at points of the mesh. These mesh functions are to be solutions of finite difference equivalents of (2), namely:

$$\left.\begin{array}{ll} (7a) \qquad & L_\delta \overline{\alpha}(x_i) = - \overline{\alpha}(x_i)\, \overline{\gamma}(x_i) - P\, x_i^2 \\ (7b) \qquad & L_\delta \overline{\gamma}(x_i) = \frac{1}{2}\, \overline{\alpha}^2\, (x_i) \end{array}\right\} \quad 0 < i < m \quad .$$

Here the difference operator, L_δ, obtained by replacing derivatives in the differential operator L by centered difference quotients, is defined for any mesh function

$\phi(x_i)$ by

$$L_\delta \phi(x_i) \equiv \frac{x_i}{(\delta x)^2} \left\{ \frac{1}{x_i + \frac{1}{2}\delta x} [x_{i+1}\phi(x_{i+1}) - x_i\phi(x_i)] - \frac{1}{x_i - \frac{1}{2}\delta x} [x_i\phi(x_i) - x_{i-1}\phi(x_{i-1})] \right\} .$$

At the endpoints, $i = 0$ and m, the mesh functions must satisfy numerical equivalents of the boundary conditions (3) and (4), say[1]

$$\text{(8a)} \qquad \overline{\alpha}(x_0) = \overline{\gamma}(x_0) = 0 \quad ,$$

and

$$\text{(8b)} \qquad \begin{aligned} a[\overline{\alpha}(x_m) - \overline{\alpha}(x_{m-1})] + \delta x \; b \; \overline{\alpha}(x_m) &= 0 \quad , \\ c[\overline{\gamma}(x_m) - \overline{\gamma}(x_{m-1})] + \delta x \; d \; \overline{\gamma}(x_m) &= \delta x \; F \quad . \end{aligned}$$

Equations (7) and (8) are a system of $2m$ non-linear algebraic equations for the determination of the $2m$ unknowns $[\overline{\alpha}(x_i), \overline{\gamma}(x_i)]$. The solution of this algebraic problem is assumed to give a "good" approximation to the functions $[\alpha(x), \gamma(x)]$ for sufficiently small δx. Indeed it can be proved, in some cases [10], that the mesh functions converge as $\delta x \longrightarrow 0$ to the solution of the continuous problem.

---

[1] Conditions (8b) may be replaced by corresponding ones centered at $x = x_m - \delta x/2$.

As the non-linear algebraic equations (7) cannot, in general, be solved explicitly we seek iterative solutions. Starting from some initial estimate, $[\bar{\alpha}_0(x_i), \bar{\gamma}_0(x_i)]$, of the mesh functions for any value of P, a simple iterative procedure is to define a sequence of mesh functions $\left\{\bar{\alpha}_n(x_i), \bar{\gamma}_n(x_i)\right\}$ by the recursions

$$\left.\begin{aligned} &(9a) \quad L_\delta \bar{\alpha}_n(x_i) = -\bar{\alpha}_{n-1}(x_i)\,\bar{\gamma}_{n-1}(x_i) - Px_i^2 \\ &(9b) \quad L_\delta \bar{\gamma}_n(x\ ) = \tfrac{1}{2}\,\bar{\alpha}_n^2(x_i) \end{aligned}\right\}\quad 0 < i < m \quad .$$

Each set of iterates is to satisfy (8) at the endpoints, $i = 0, m$. For each n, equations (9a) now form a system of $(m-2)$ linear equations in the $(m-2)$ unknowns, $\bar{\alpha}_n(x_i)$, $i \neq 0, m$. These equations may be solved explicitly in a simple manner.[2] The same is then true of the system (9b) and the $\bar{\gamma}_n(x_i)$ may also be obtained explicitly. The convergence as $n \longrightarrow \infty$ of this simple iteration procedure has been examined in detail [10] for application to problems A), B) and C). A summary of this analysis is contained in the Appendix. For these cases it is proved that the iterations converge only for a limited range of load parameters, $0 \leq P < P'$, (see Table I in Appendix) and that they actually diverge for sufficiently large values of the parameter $P \geq P^{**}$. (Analogous results can be obtained for the buckling problems D and E.) Since solutions for loads $P >> P^{**}$ are of primary interest we discard the simple iterative procedure and seek one that converges for an unlimited range of P.

---

[2] The coefficient matrix of this system is of Jacobi or "triple diagonal" form. Such a matrix can be factored into the product of an upper- by a lower-triangular matrix. The only non-zero elements of these factors lie on the diagonal or immediately to its right or left respectively. The solution of the system is then obtained by evaluating two two-term recursions.

A new iterative procedure is suggested by examining a physical explanation of the divergence of the iterations (9). Each iterate, $\overline{\alpha}_n(x_i)$, may be thought of as the solution for a plate under a "non-uniform normal load" in the linear theory of bending. This load consists of the uniform lateral pressure P plus a non-uniform "normal force" resulting from the slope and membrane stress given by the previous iterate, $[\overline{\alpha}_{n-1}(x_i), \overline{\gamma}_{n-1}(x_i)]$. The stress function, $\overline{\gamma}_n(x_i)$, is a result of the deflection determined by $\overline{\alpha}_n(x_i)$. Now, physically, if the "non-uniform load" induced by a given iterate is everywhere larger in absolute magnitude than the corresponding load which produced this given iterate, the sequence should diverge. (This is shown to be the case in [10] and in the Appendix when $P \geq P^{**}$.) Thus it may be possible to eliminate divergence by properly correcting (9a) for over-estimates in the next iterate. We attempt such a correction by introducing the provisional iterate $\overline{\alpha}_n^*(x_i)$, as in (9a), by

$$(10a) \qquad L_\delta \overline{\alpha}_n^*(x_i) = - \overline{\alpha}_{n-1}(x_i)\, \overline{\gamma}_{n-1}(x_i) - Px_i^2 \;, \quad 0 < i < m \quad ,$$

and then interpolating between it and the previous iterate to obtain

$$(10b) \qquad \overline{\alpha}_n(x_i) = \theta \overline{\alpha}_n^*(x_i) + (1 - \theta)\overline{\alpha}_{n-1}(x_i) \quad .$$

Here θ is an interpolation parameter which must lie in the range $0 < \theta \leq 1$. The iterates $\overline{\gamma}_n(x_i)$ are defined again by (9b) and both iterates are to satisfy (8) at the endpoints of the mesh. The solution of the equations for the interpolated iterate case can be obtained just as in the simple iteration case since similar linear equations need be solved. It is clear that taking $\theta = 1$ in (10b) reduces the interpolated procedure to the simple iteration (9).

The convergence of the interpolated iterates (10), (9b) and (8), for proper choices of θ and initial iterates, $[\overline{\alpha}_0(x_i), \overline{\gamma}_0(x_i)]$, is made plausible in [10]. An empirical method for determining proper values of θ is presented in the next section and a theoretical bound on θ is given in [10]. The proposed numerical procedure is then well suited for application on automatic computing machines.

4. Computational Procedures.

In applying the difference equations (7) it is required that the mesh spacing, δx, be "sufficiently small." We determined a satisfactory value from a series of test calculations with successively finer meshes, say $\delta x = 0.1$, 0.05 and 0.02. From these tests it was observed that the .02 mesh provided accurate solutions for the ranges of loads considered.

Application of the iteration scheme (10), (9b) to solve the difference equations (7) requires procedures for determining an initial iterate, a "best" value for Θ and a criterion for convergence of the iterates. For the latter we use

$$(11) \quad \max_{0 \leq i \leq m} \left\{ |\overline{\alpha}_n(x_i) - \overline{\alpha}_{n-1}(x_i)| \;,\; |\overline{\gamma}_n(x_i) - \overline{\gamma}_{n-1}(x_i)| \right\} < 10^{-5} \;,$$

and iterate until this condition is satisfied. It is found that the number of iterations required, starting from a given initial iterate, depends strongly upon the value of Θ used in (10b). A typical graph of this dependence of the number of iterations for convergence, $N(\Theta)$, on Θ for a given value of the load parameter is shown in Fig. 1. The "best" value of Θ, is that value, Θ_{op}, for which $N(\Theta)$ is a minimum. From such graphs for a sequence of values of the load parameter, say P, a corresponding sequence of values of $\Theta_{op}(P)$ is obtained. From a smooth curve through the points $(P,\Theta_{op}(P))$ good estimates of Θ_{op} for an entire range of load may be determined (see Fig. 2). It was found that Θ_{op} does not change appreciably for significant changes in δx and thus curves of $\Theta_{op}(P)$ were determined with few mesh points and little computing time. A graph of $\Theta_{op}(P)$ for problem A) is shown in Fig. 2, together with a theoretical upper bound determined in [10]. Similar graphs have been obtained for the other problems.

The initial iterate for a given load P in any of the bending problems, A), B) or C), is taken to be the final ("converged") iterate for a slightly smaller value of load, that is

$$\bar{\alpha}_0(P,x_i) = \bar{\alpha}_N(P - \delta P,x_i) \quad .$$

In this manner solutions were obtained, with the aid of the previously estimated $\Theta_{op}(P)$, for an apparently unlimited range of load.

The buckling problems, D) and E), have non-unique solutions and so the above procedure must be applied with care. It has been shown by Friedrichs and Stoker [3,4] that for $F < F_0$ (where F_0 is the first eigenvalue of the linear buckling problem) the only solution is the trivial one: $\alpha(x) = 0$, $\gamma(x) = Fx$. For $F \geq F_0$ two solutions [that differ from each other only in the sign of $\alpha(x)$] in addition to the trivial one are possible. If the trivial solution is used as an initial iterate it might then result as the solution for all F and the non-trivial solutions would not be detected. To avoid this possibility we use the non-zero initial iterate $\bar{\alpha}_0(x_i) = x_i$ for some $F < F_0$ and the iterations then converge to the trivial solution. This procedure is continued for a sequence of increasing values of F until a non-trivial solution is obtained. This non-trivial solution is then used as the initial iterate for the next value of F and the procedure is continued as in the bending problems. In this manner a knowledge of the value of F_0 is not required and it can in fact be estimated from the computations. It is also found that the value of $\theta_{op}(F)$ for obtaining trivial solutions when $F < F_0$ is greater than one and extrapolation is automatically used in (10b). Near $F = F_0$, $\theta_{op}(F) \approx 1$ and as the non-trivial solutions are obtained for increasing F, $\theta_{op}(F)$ decreases. Thus it would seem that the curve of $\theta_{op}(F)$ has a bifurcation, as do the solutions, at F_0.

When the iterations converge for a given load the stresses and deflections can be computed. For this purpose we employ obvious finite difference equivalents of equations (1) and (3) and evaluate them using the final iterates, $\{\bar{\alpha}_N(x_i), \bar{\gamma}_N(x_i)\}$. Such results are presented and discussed in the next section.

5. Discussion of Results.[3]

Representative[4] graphs of the reduced stresses and deflections as functions of x for increasing sequences of load are presented in Fig's. (3a-e) for bending problem C), and in Fig's. (4a-e) for buckling problem E). Similar results have been obtained for the other three problems and those of problem A) are presented in [10].

In Fig. 3b, the reduced slope, α, for problem C) is shown to have a maximum near the edge. Although it is not obvious from the curves, the data indicates that the location of this maximum moves towards the edge as P increases. The reduced circumferential membrane stress (Fig. 3c) remains tensile and rather flat in the center of the plate and changes rapidly to compressive with its maximum at the edge. The point of zero stress moves toward the edge with increasing P. This sharp transition of the stress near the edge from tensile to compressive is characteristic of the "boundary layer" behavior first discovered by Friedrichs and Stoker [3,4]. The radial membrane stress (not shown) has a graph similar to the lateral deflection W of Fig. 3a with a maximum at the center. It can be observed from these graphs that

---

[3] All the numerical calculations were performed on the Atomic Energy Commission UNIVAC at NYU. The authors wish to express their appreciation to M. Weissner, I. Krongold and S. Weinberg for their aid in coding these problems for the machine.

[4] In all calculations Poisson's ratio, $\nu = .3$.

$$(12) \qquad \max|\Sigma_C| > \max|\Sigma_R| \quad .$$

For low values of P, the bending stresses, Fig's. (3d,e), have their maxima at the center of the plate. As P increases these points of maximum stress move toward the edge thus again exhibiting a boundary layer behavior. In addition we observe that

$$(13) \qquad \max|\Sigma_C| > \max|\Sigma_R^B| \geq \max|\Sigma_C^B| \quad ,$$

where the equality holds only when the maximum bending stresses are at the center. Hence the dominant stress is the circumferential membrane stress at the edge.

The curves for bending problem A) are presented in [10]. Here the graphs of α clearly show that the location of the maxima move towards the edge as P increases. Both membrane stresses remain tensile with their maxima at the center and nence their maxima are equal. The bending stresses are tensile and almost constant in the central portion of the plate and rapidly change to compressive and maximum at the edge. Again the points of zero stress approach the edge with increasing P. The dominant stress in this problem is the radial bending stress at the edge of the plate.

For problem B) the graphs of the slope and bending stresses are similar to those of problem C) and the membrane stresses are similar to those of problem A). The maxima of all the stresses are related as in (13).

The reduced lateral deflection and slope for buckling problem E) (see Fig's. 4a,b) flatten in the central portion of the plate as F increases. Thus in this central region the slope approaches zero while in the bending problems the slope increases as the load parameter increases. For F slightly larger than the critical value the membrane stresses (see Fig. 4c) are tensile in the central region and flatten in this region as F increases. These stresses rapidly decline and become compressive reaching a maximum at the edge (for the radial stress) or near the edge (for the circumferential stress). The maxima of the membrane stresses are related as in (12). The bending stresses are tensile in the central region reaching a tensile maximum near the edge and then rapidly decreasing to compressive with the maximum at the edge, see Fig's. (4d,e). These stresses approach zero with increasing F, in the central region, and both the locations of tensile maximum and zero stress move towards the edge. Although

$$\max |\Sigma_C| \doteq \max |\Sigma_R^B|$$

equations (3) show that

$$\max |\sigma_R^B| > \max |\sigma_C| \quad .$$

Hence $\max |\sigma_R^B|$ is the dominant stress.

The graphs of lateral deflection (W), slope (α), radial membrane stress (Σ_R) and circumferential membrane stress (Σ_C) for problem D) are very similar to those for problem E). However the bending stresses are always tensile with the maximum moving toward the edge as F increases. The dominant stress is the circumferential membrane stress at the edge. These results for problem D) are in good agreement with those of Friedrichs and Stoker [4].

Figures 5a-e are graphs of the load parameter vs. the lateral deflection at the center and the maximum membrane and bending stresses for each of the five problems.

To compare methods power series solutions [2,5] were computed on the UNIVAC for problem A). All of these solutions are in excellent agreement with those obtained by the iteration method presented in this paper. However the power series method has two distinct disadvantages: the computing time it requires far exceeds that for the present method; power series solutions could be obtained only for $P \leq 2000$. The present method easily yields solutions for loads as high as $P = 7000$ and it seems unlimited in this respect.

In computing the ultimate load of a buckled rectangular plate it is customary [11] to assume that in the post-buckling region the entire load is resisted by two narrow strips adjacent to the edges parallel to the loading. In these strips it is further assumed that the stress normal to the width, i.e. in the direction of loading, is constant and equal to the edge stress. The width of these strips, which must be determined, is commonly referred to as the "effective width." The concept of effective width is clearly related to the boundary layer and its characteristics in the neighborhood of the edge. In fact some measure of the "boundary layer thickness" may be considered to be the effective width and conversely.

From the results for the circular plate it is possible to gain some insight into appropriate measures of the boundary layer thickness. From analogy with the rectangular plate we may assume in this case that the stresses perpendicular to the boundary layer, the circumferential stresses, are of primary importance. For example in problem E), Fig's. (4c and e), the distance from the edge to the point of zero circumferential stress, which decreases with increasing F, may be taken as a measure of the boundary layer thickness. This distance is plotted as a function of F in Fig. 6. From these graphs empirical formulae for the variation of the thickness with F can be obtained. Alternate definitions determined by other characteristics of the boundary layer could have been employed.

BIBLIOGRAPHY

[1] von Kármán, T., *Festigkeitsprobleme im Maschinenbau*, Encyklopädie der mathematischen Wissenschaften, Vol. IV, 4, Teubner, Leipzig, 1910, pp. 348-352.

[2] Way, S., *Bending of Circular Plates with Large Deflection*, Trans. A.S.M.E., Vol. 56, 1934, pp. 627-636.

[3] Friedrichs, K. O., and Stoker, J. J., *The Non-Linear Boundary Value Problem of the Buckled Plate*, Amer. J. of Math., Vol. 63, 1941, pp. 839-888.

[4] Friedrichs, K. O., and Stoker, J. J., *Buckling of the Circular Plate beyond the Critical Thrust*, J. Appl. Mech., Vol. 9, 1942, pp. A7-A14.

[5] Bromberg, E., *Non-Linear Bending of a Circular Plate under Normal Pressure*, Comm. Pure and Appl. Math., Vol. 9, 1956, pp. 633-659.

[6] Chien, W. Z., *Large Deflection of a Circular Clamped Plate under Uniform Pressure*, Chin. Journ. of Phys., Vol. 7, 1947, pp. 102-114.

[7] Chien, W. Z., *Asymptotic Behavior of a Thin Clamped Circular Plate under Uniform Normal Pressure at Very Large Deflection*, Sci., Rep. Nat. Tsing Hua Univ., Sec. A, Vol. 5, 1948, pp. 71-94.

[8] Bodner, S. R., *The Post Buckling Behavior of a Clamped Circular Plate*, Quart. Appl. Math., Vol. 12, 1954, pp. 397-401.

[9] Green, J. R., and Southwell, R. V., *Relaxation Methods Applied to Engineering Problems IIIA. Problems Relating to Large Transverse Displacements of Thin Elastic Plates*, Phil. Trans. Roy. Soc., *A*, Vol. 239, 1945, pp. 539-78.

[10] Keller, H. B., and Reiss, E. L., Iterative Solutions for the Non-Linear Bending of Circular Plates, to appear in Comm. Pure and Appl. Math., Vol. XI, No. 3, 1958.

[11] von Kármán, T., Sechler, E. E., and Donnell, L. H., The Strength of Thin Plates in Compression, Trans. A.S.M.E., Vol. 54, 1932, pp. APM-54-5.

APPENDIX: Theoretical Convergence Properties.

In this section a summary of the convergence properties of the simple iteration procedure is presented. Only the bending problem A will be considered. All results obtained for this case have exact analogies for the other bending problems, B and C, and a similar analysis can be carried out for the buckling problems D and E.

The formulation given by (2), (4) and (5)A) can be replaced by the equivalent integral equations

$$\text{(A.1)}\qquad \begin{aligned} \alpha(x) &= f(x) - \int_0^1 g_1(x,\xi)\alpha(\xi)\gamma(\xi)d\xi \quad , \\ \gamma(x) &= \frac{1}{2}\int_0^1 g_2(x,\xi)\alpha^2(\xi)d\xi \quad ; \end{aligned}$$

where

$$\text{(A.2)}\qquad f(x) \equiv \frac{P}{8}\, x(1-x^2) = \int_0^1 g_1(x,\xi)P\xi^2 d\xi \quad ;$$

and

$$\text{(A.3)}\qquad \begin{aligned} g_1(x,\xi) &\equiv -\frac{1}{2}\begin{cases} (\frac{1}{x} - x)\xi & \xi \le x \quad , \\ x(\frac{1}{\xi} - \xi) \quad , & \xi \ge x \quad ; \end{cases} \\ g_2(x,\xi) &\equiv -\frac{1}{2}\begin{cases} (\frac{1}{x} + \frac{x}{\mu})\xi \quad , & \xi \le x \\ x(\frac{1}{\xi} + \frac{\xi}{\mu}) \quad , & \xi \ge x \end{cases} \quad , \ \mu \equiv \frac{1 - \nu}{1 + \nu} \end{aligned}$$

From the differential equations and the fact that $g_1(x,\xi)$ and $g_2(x,\xi) \leq 0$ for $0 \leq x,\xi \leq 1$ we may conclude that

$$\begin{aligned} & 0 \leq \alpha(x) \leq f(x) \\ \text{(A.4)} \quad & 0 \geq \gamma(x) \geq g(x) = \frac{1}{2}\int_0^1 g_2(x,\xi)f^2(\xi)d = -\left(\frac{P}{8}\right)^2\frac{x}{96} \\ & \qquad\qquad [(4 + \frac{1}{\mu})-x^2(6-4x^2+x^4)] \end{aligned}$$

These are bounds on the exact solution and are valid for all loads.

The n-th iterate of the numerical procedure (9) is a numerical approximation of the n-th iterate of the analytical iteration scheme defined by: $\alpha_0(x) = 0$,

$$\begin{aligned} & L\,\alpha_n(x) = -\alpha_{n-1}(x)\gamma_{n-1}(x) - Px^2 \\ \text{(A.5)} \quad & L\,\gamma_n(x) = \frac{1}{2}\,\alpha_n^2(x) \end{aligned}$$

where each iterate is to satisfy the boundary conditions (5)A). Since the solutions of these equations are sufficiently smooth it can be proven that the numerical solutions of (9) converge as $\delta x \longrightarrow 0$ to the solution of (A.5). Thus the convergence of the numerical iterations (as $n \longrightarrow \infty$) is equivalent to the convergence of the analytic iterations.

The solution of (A.5) is, in terms of the Green's functions (A.3),

$$
\text{(A.6)} \qquad
\begin{aligned}
\alpha_n(x) &= f(x) - \int_0^1 g_1(x,\xi)\alpha_{n-1}(\xi)\gamma_{n-1}(\xi)d\xi, \\
\gamma_n(x) &= \frac{1}{2}\int_0^1 g_2(x,\xi)\alpha_n^2(\xi)d\xi \quad .
\end{aligned}
$$

If $\alpha_2(x) \geq 0$ for $0 \leq x \leq 1$ we may then prove by induction that

$$
\text{(A.7)} \qquad
\left.
\begin{aligned}
0 &\equiv \alpha_0 \leq \alpha_2 \leq \cdots \leq \alpha_{2n} \leq \cdots\cdots \leq \alpha_{2n+1} \leq \cdots\cdots \leq \alpha_1(x) \equiv f(x) \\
0 &\equiv \gamma_0 \geq \gamma_2 \geq \cdots \geq \gamma_{2n} \geq \cdots\cdots \geq \gamma_{2n+1} \geq \cdots\cdots \geq \gamma_1(x) \equiv g(x)
\end{aligned}
\right\} 0 \leq x \leq 1.
$$

The bounds of these sequences are just the bounds (A.4) on the exact solution. By a simple calculation it can be shown that $\alpha_2(x) \geq 0$ if $P \leq P^*$, where P^* can be explicitly evaluated (see Table I).

If $\alpha_2(x) \leq 0$ for all $0 \leq x \leq 1$ the iterations (A.6) must diverge, forming the sequences

$$
\text{(A.8)} \qquad
\begin{aligned}
\cdots\cdots \leq \alpha_{2n} \leq \cdots\cdots \leq \alpha_2 \leq \alpha_0 \leq \alpha_1 \leq \cdots\cdots \leq \alpha_{2n+1} \leq \cdots\cdots \quad ; \\
\gamma_0 \geq \gamma_1 \geq \cdots\cdots \geq \gamma_{2n+1} \geq \cdots\cdots \quad ; \\
\gamma_0 \geq \gamma_2 \geq \cdots\cdots \geq \gamma_{2n} \quad \geq \cdots\cdots \quad .
\end{aligned}
$$

The previous calculation also shows that $\alpha_2(x) \leq 0$ if

$P \geq p^{**}$ (see Table I for p^{**}).

It is possible that for $P \leq P^*$ the iterates, $\alpha_n(x)$, will not converge, i.e. the even and odd subsequences in (A.7) could converge to different limiting functions. However, we can prove that there is some $P' < P^*$ such that they converge for all $P < P'$. For this proof consider $|\alpha_{n+1}(x) - \alpha_n(x)|$ and use the bounds $f(x)$ and $g(x)$ of (A.7) to derive

$$\text{(A.9)} \qquad \max_x |\alpha_{n+1}(x) - \alpha_n(x)| \leq K^n \max_x |f(x)| \quad ,$$

where

$$\text{(A.10)} \qquad K \equiv \left(\frac{P}{8}\right)^2 \max_{0 \leq x \leq 1} p_3(x) \quad ,$$

and $p_3(x)$ is a non-negative polynomial, independent of P, in $0 \leq x \leq 1$. Taking

$$\text{(A.11)} \qquad P' = 8\left[\max_{0 \leq x \leq 1} p_3(x)\right]^{-1/2} < P^* \quad ,$$

we have $K < 1$ for all $P < P'$ and hence by (A.9) the sequences (A.7) converge as $n \longrightarrow \infty$.

The values of P', P^* and P^{**} are given in Table I for problems A, B and C. A more detailed estimate

	Prob. A	Prob. B	Prob. C
P'	68.3	9.9	24.0
P*	125.3	14.9	28.3
P**	197.0	15.6	42.6

Table I

of K in deriving (A.9) would raise the values of P' above those presented in the table.

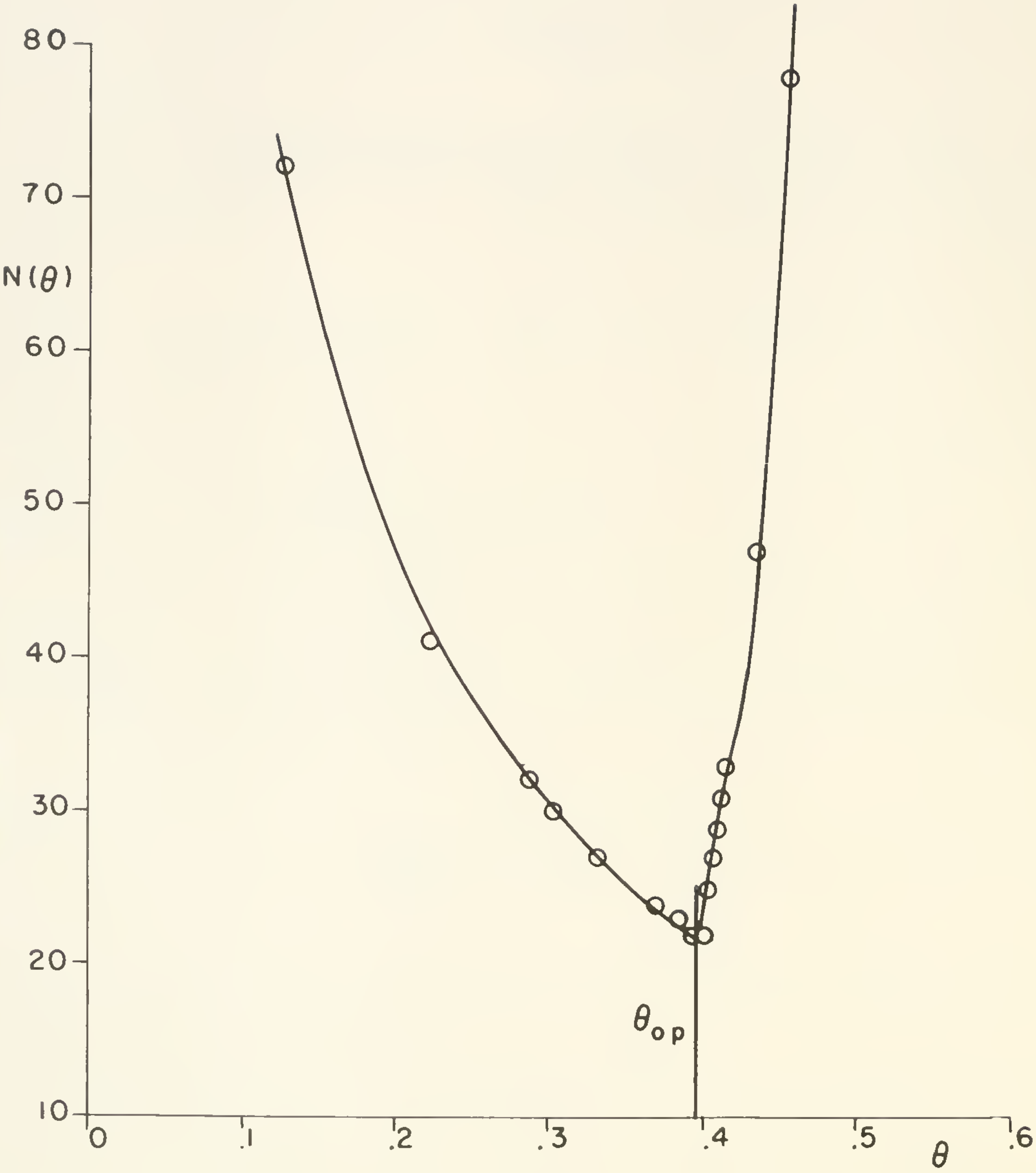

Fig. 1: Typical Graph of Number of Iterations for Convergence.

Problem A, $P = 300$, $\delta x = .05$, $a_0(x_i) = \text{const}$.

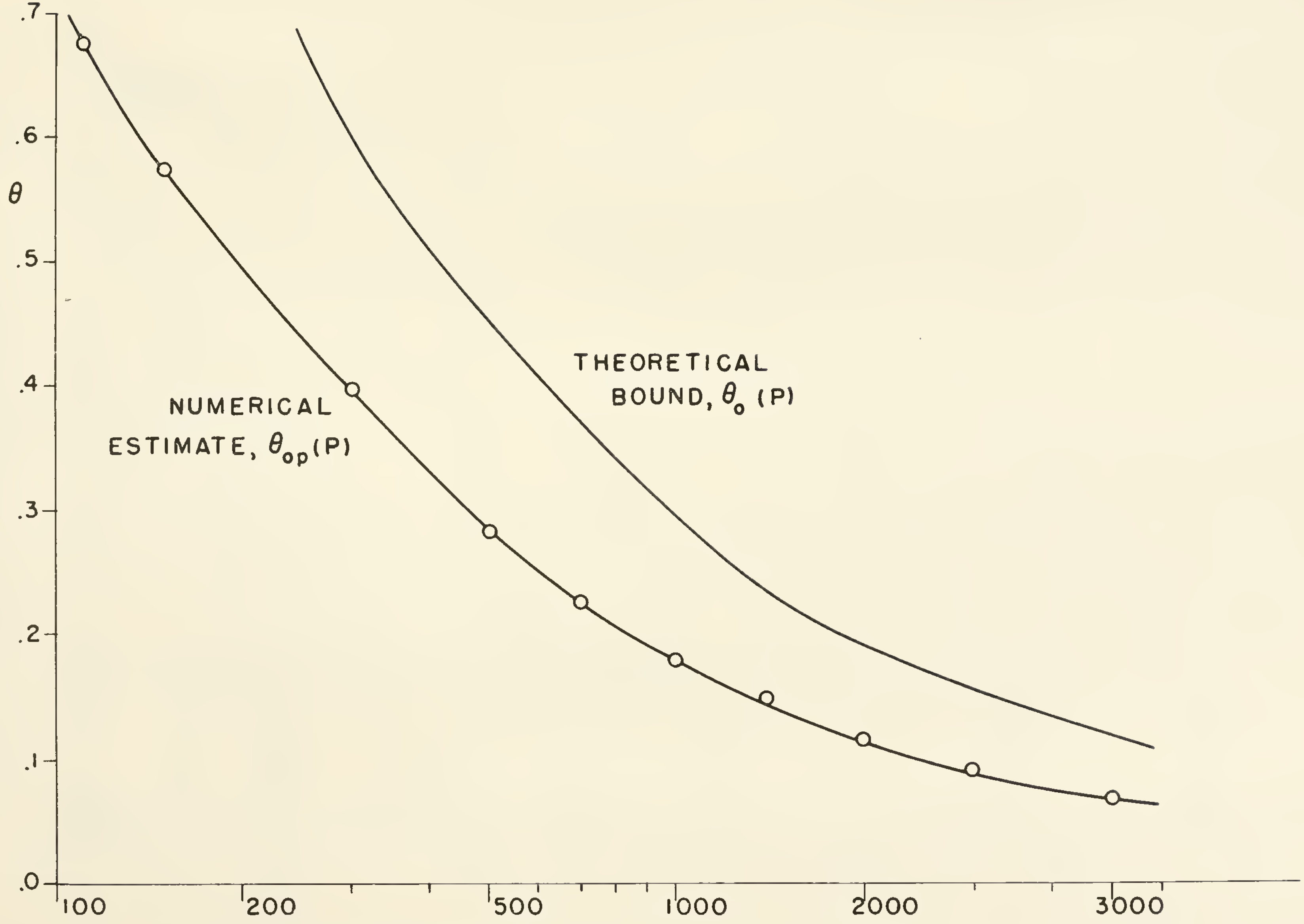

Fig. 2: Graph of Optimum θ for Problem A.

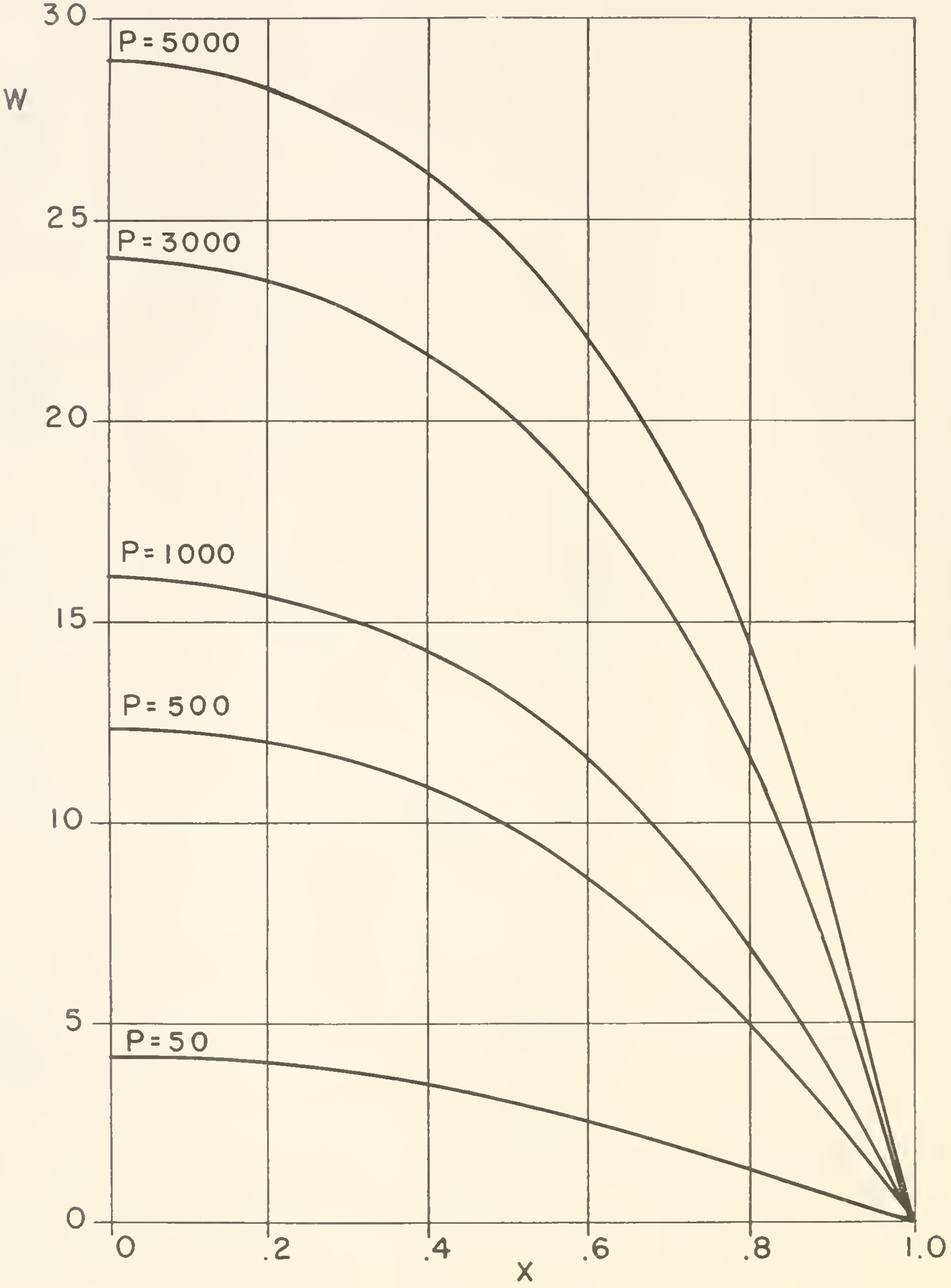

Fig. 3a: Reduced Lateral Deflection, Problem C

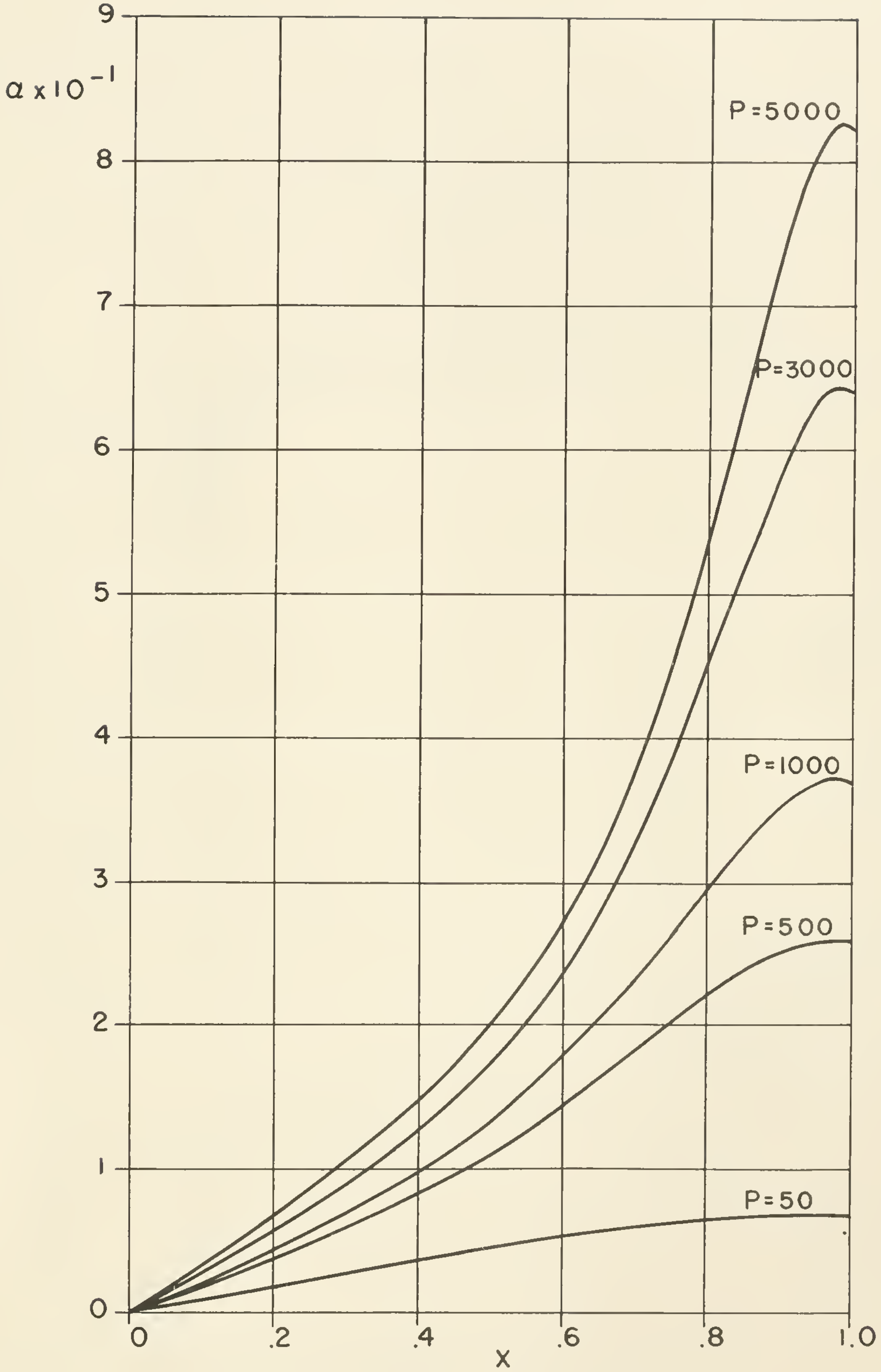

Fig. 3b: Reduced Slope, Problem C.

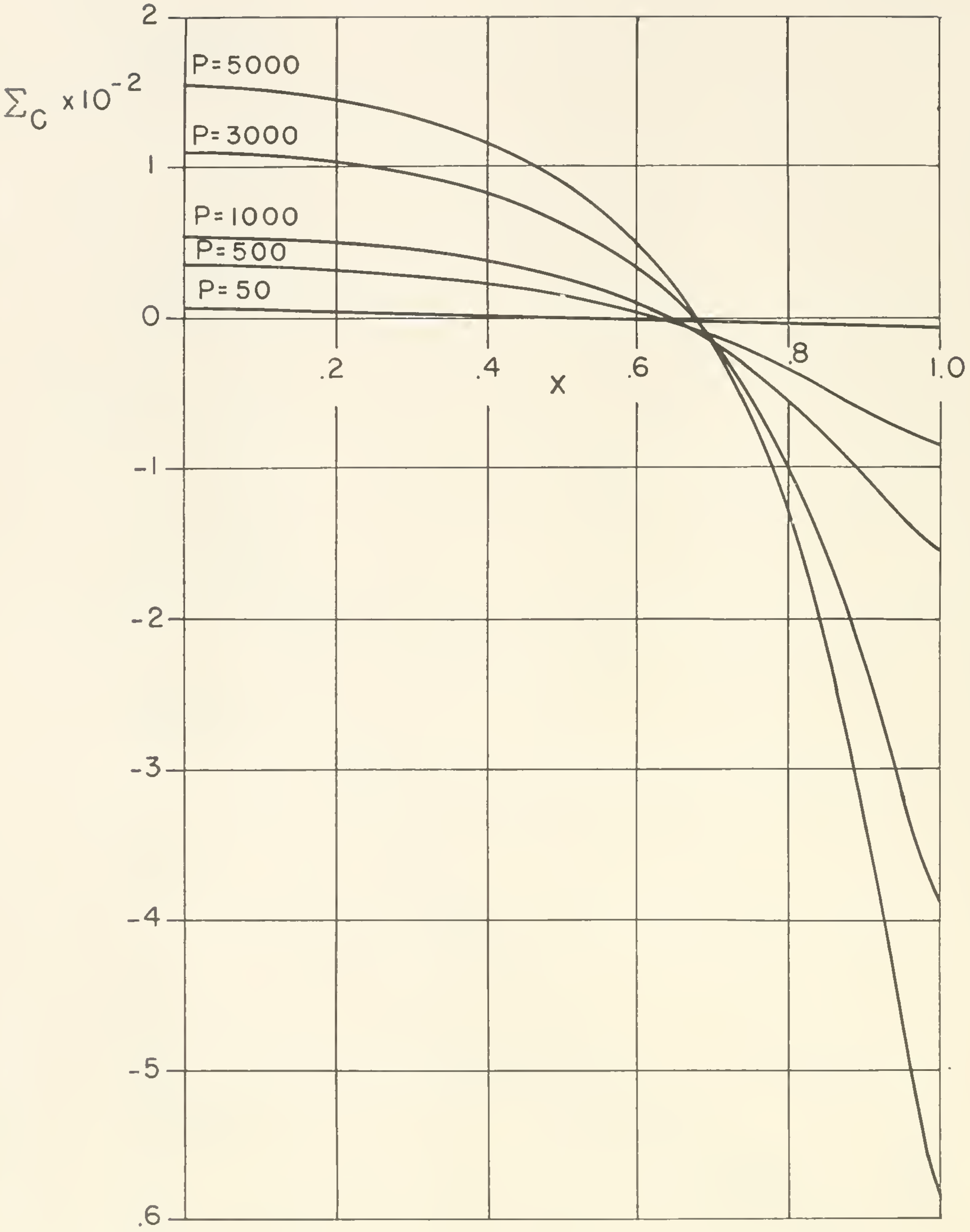

Fig. 3c: Reduced Circumferential Membrane Stress, Problem C.

Fig. 3d: Reduced Radial Bending Stress, Problem C.

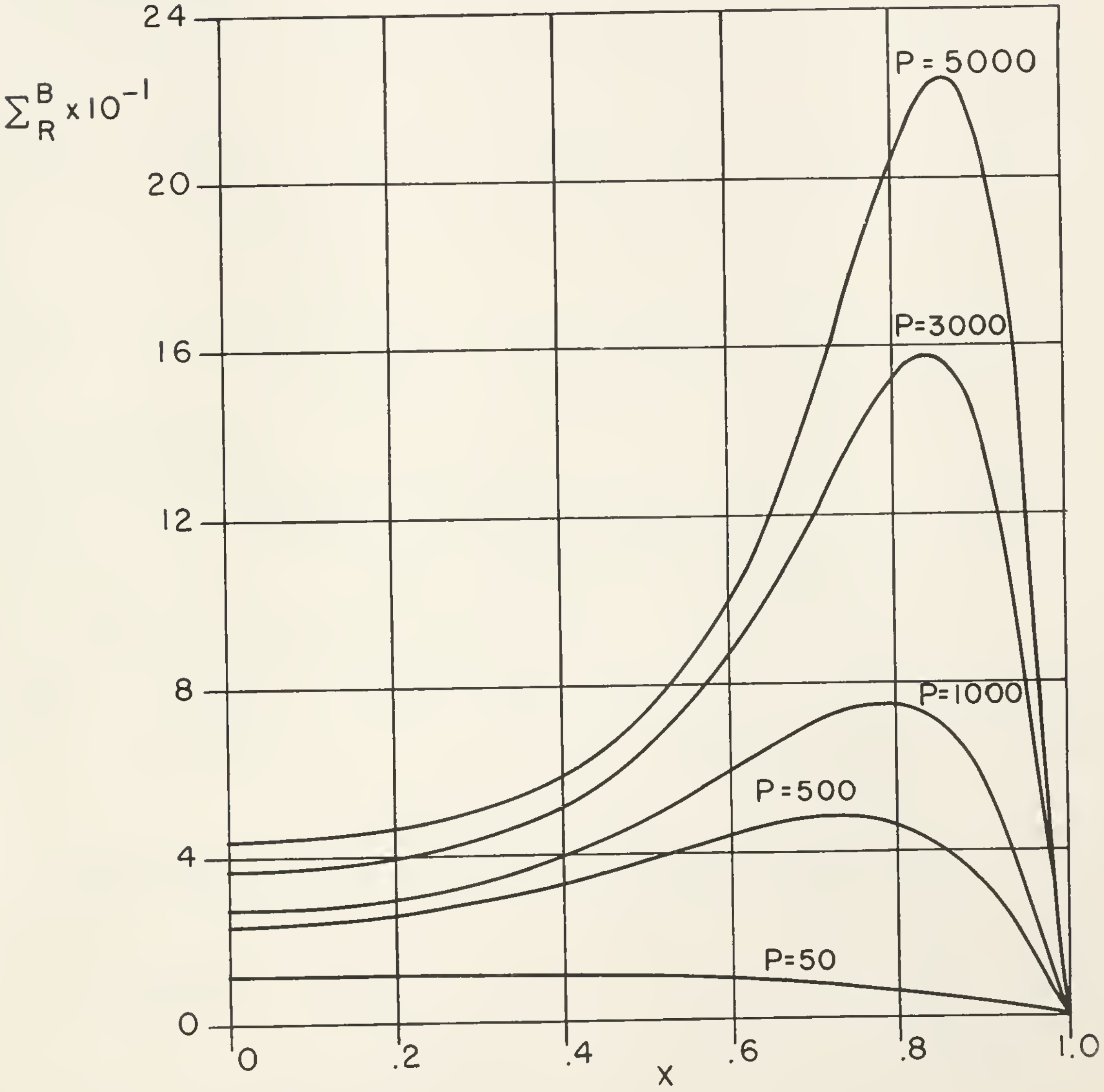

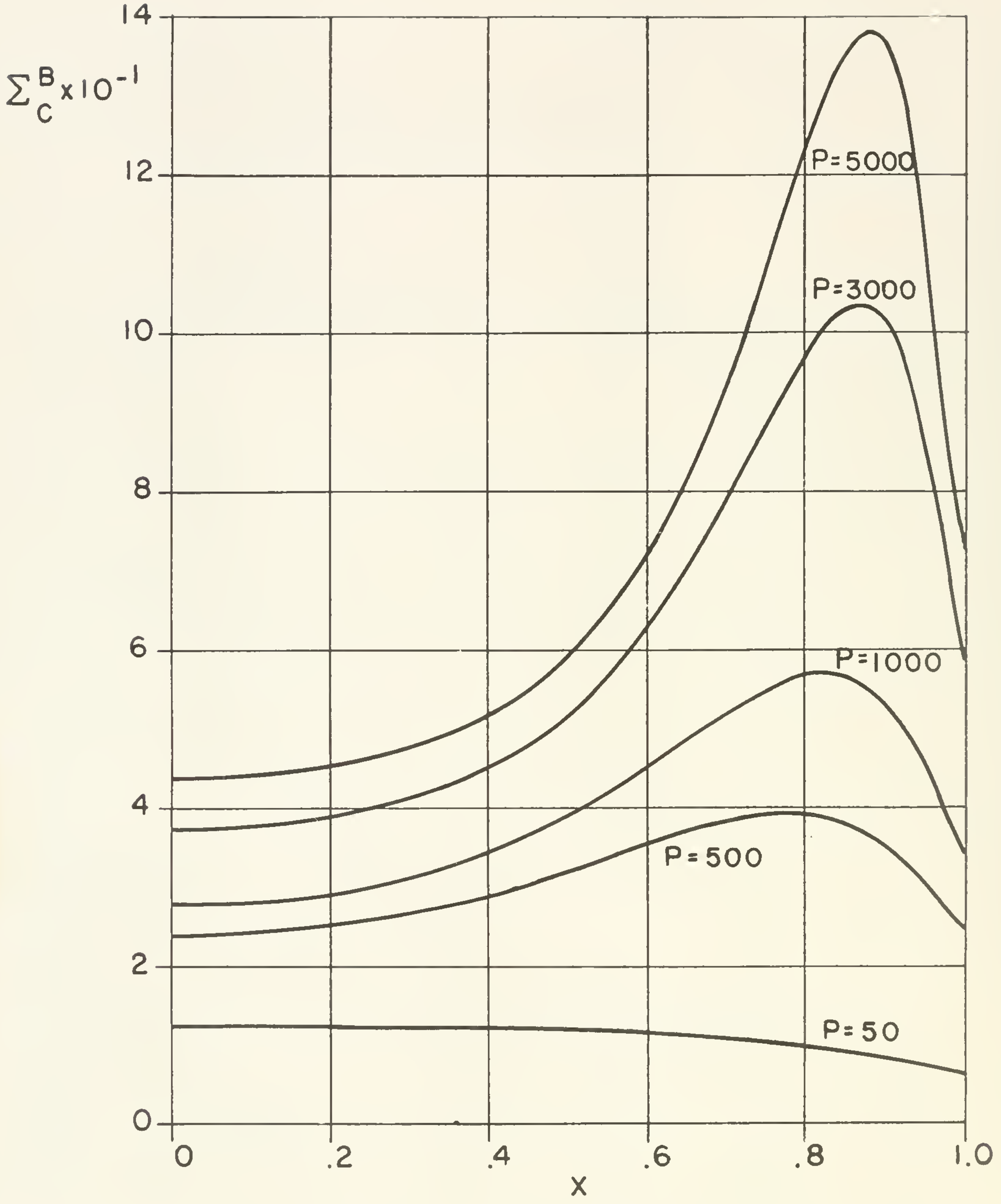

Fig. 3e: Reduced Circumferential Bending Stress, Problem C.

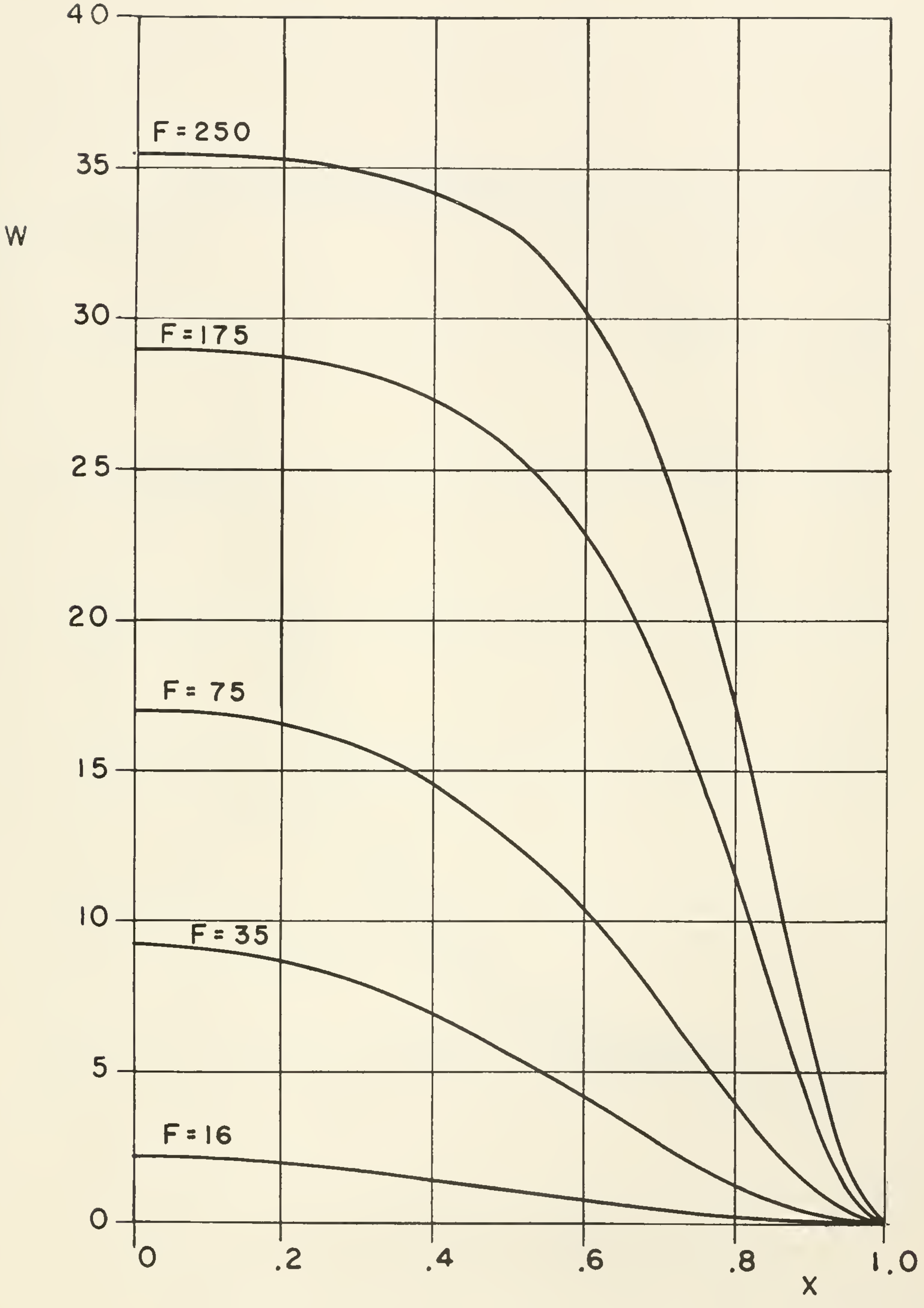

Fig. 4a: Reduced Lateral Deflection, Problem E.

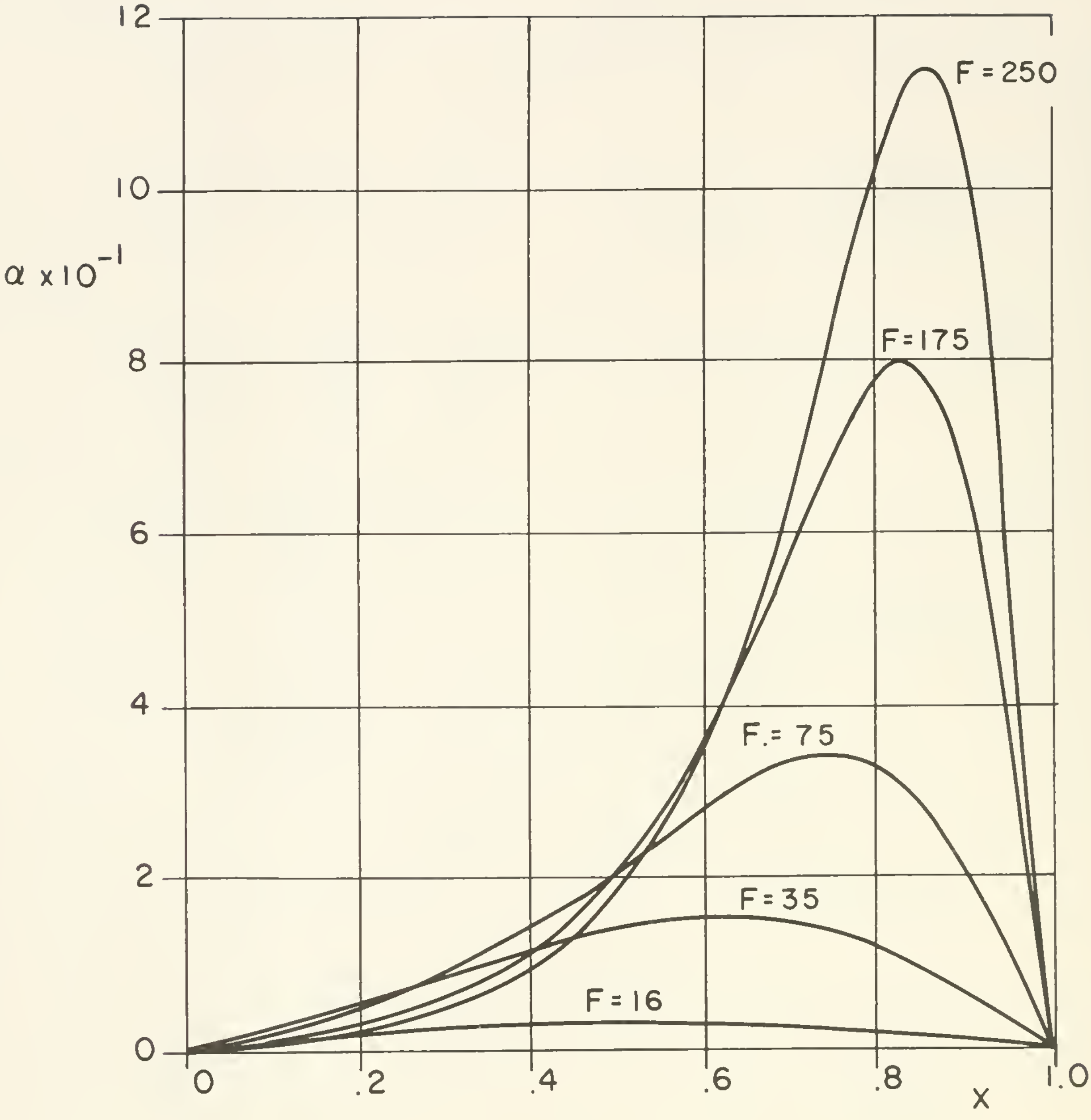

Fig. 4b: Reduced Slope, Problem E.

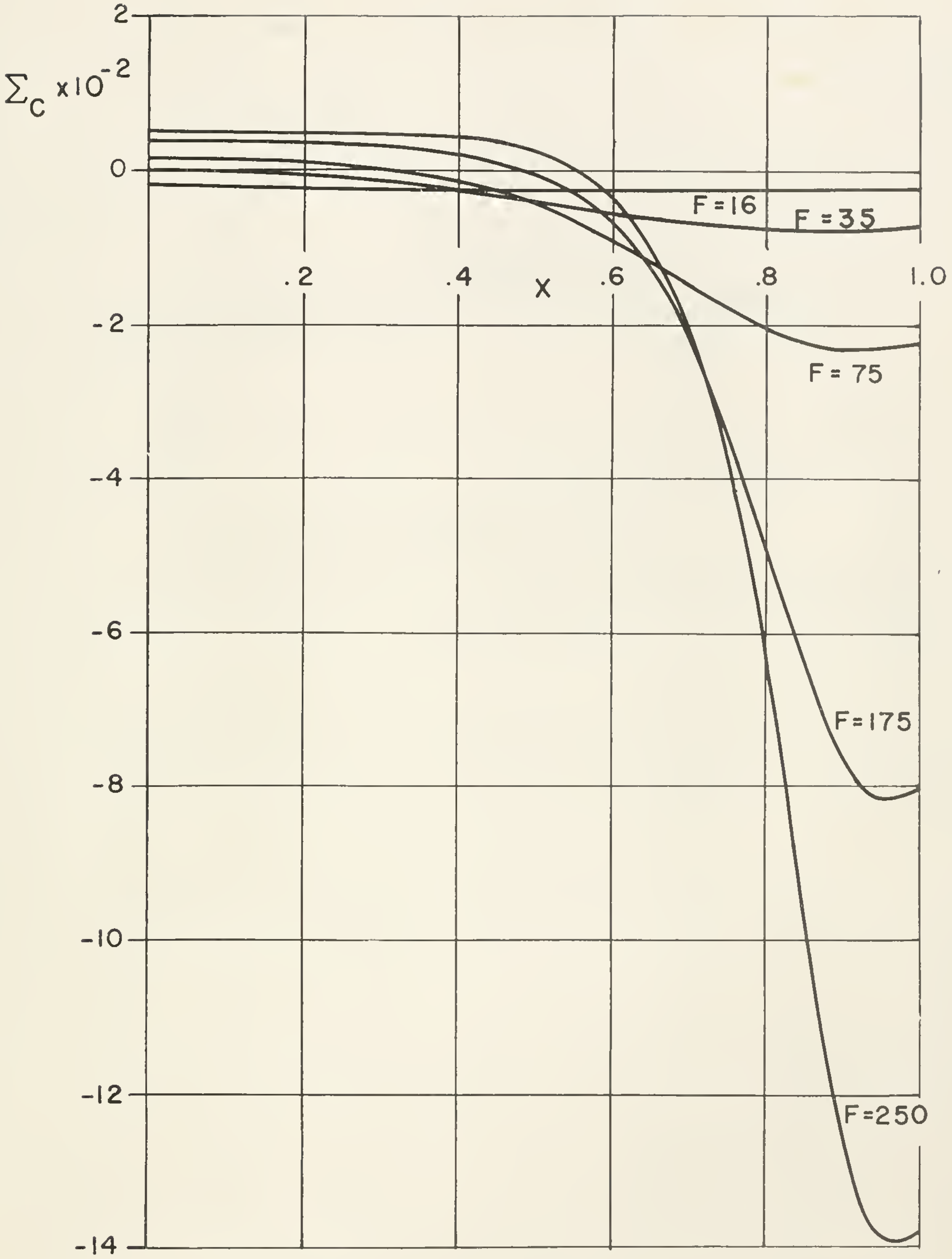

Fig. 4c: Reduced Circumferential Membrane Stress, Problem E.

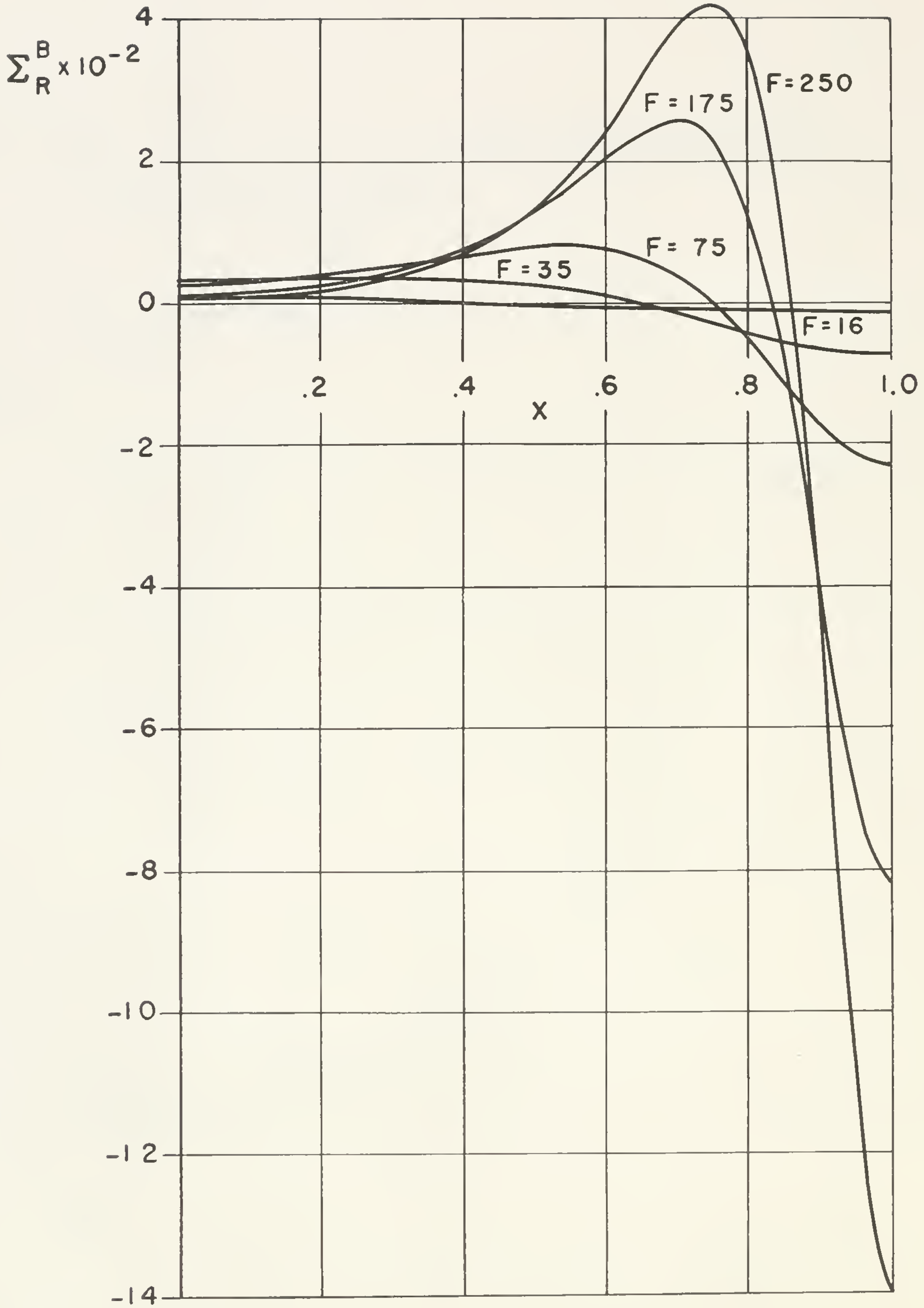

Fig. 4d: Reduced Radial Bending Stress, Problem E.

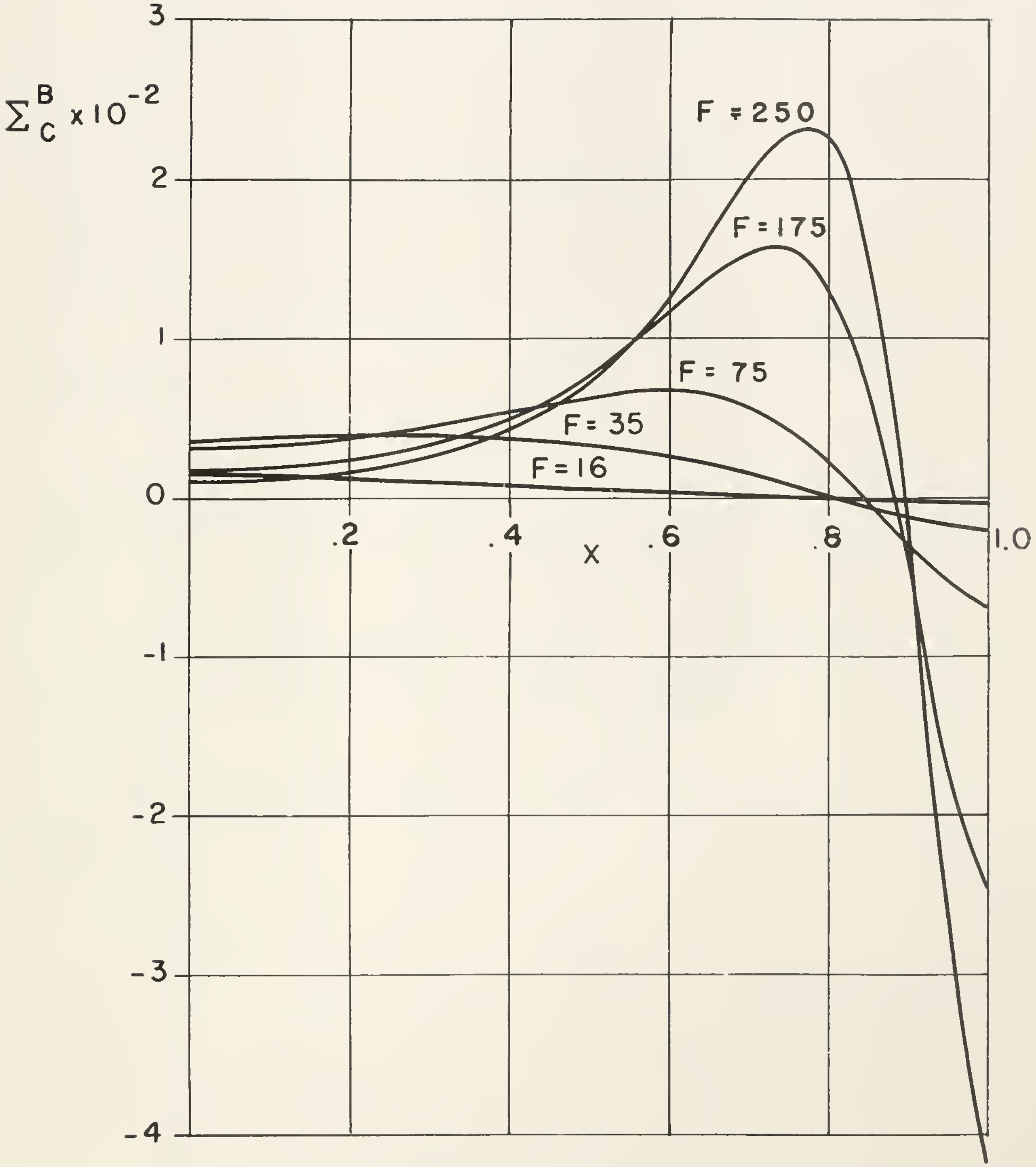

Fig. 4e: Reduced Circumferential Bending Stress, Problem E.

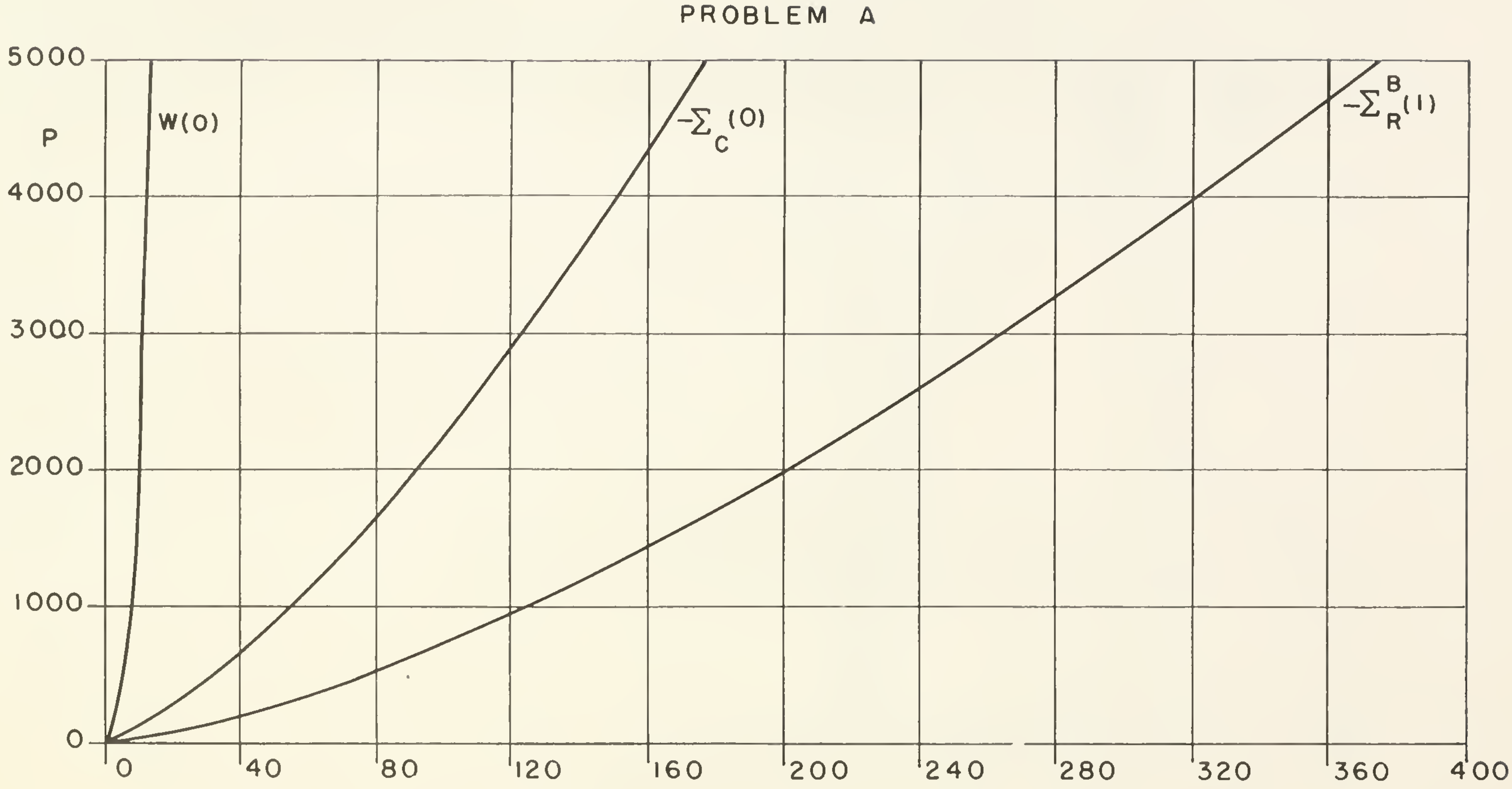

Fig. 5a: Maximum Stresses and Deflection at the Center, Problem A.

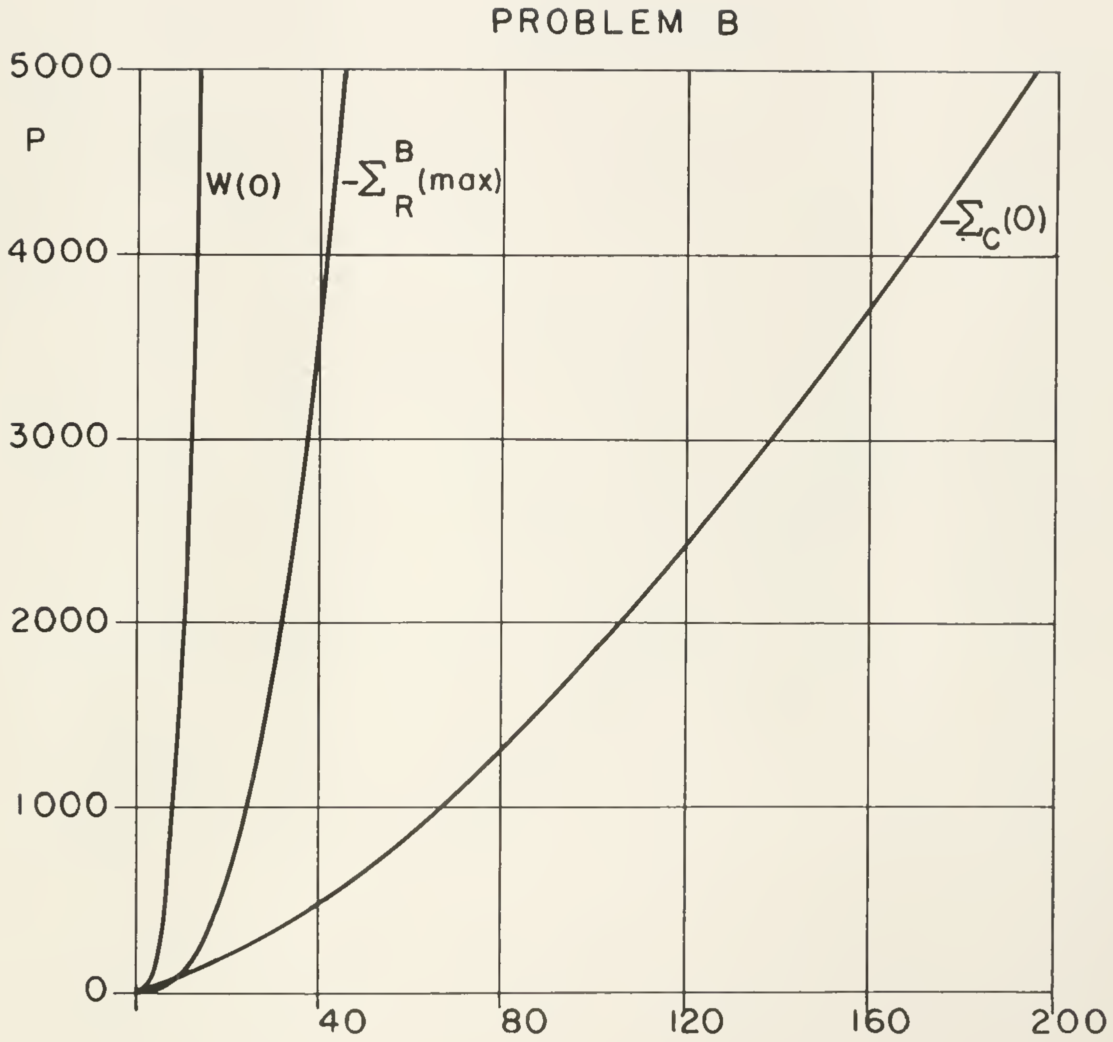

Fig. 5b: Maximum Stresses and Deflection at the Center, Problem B.

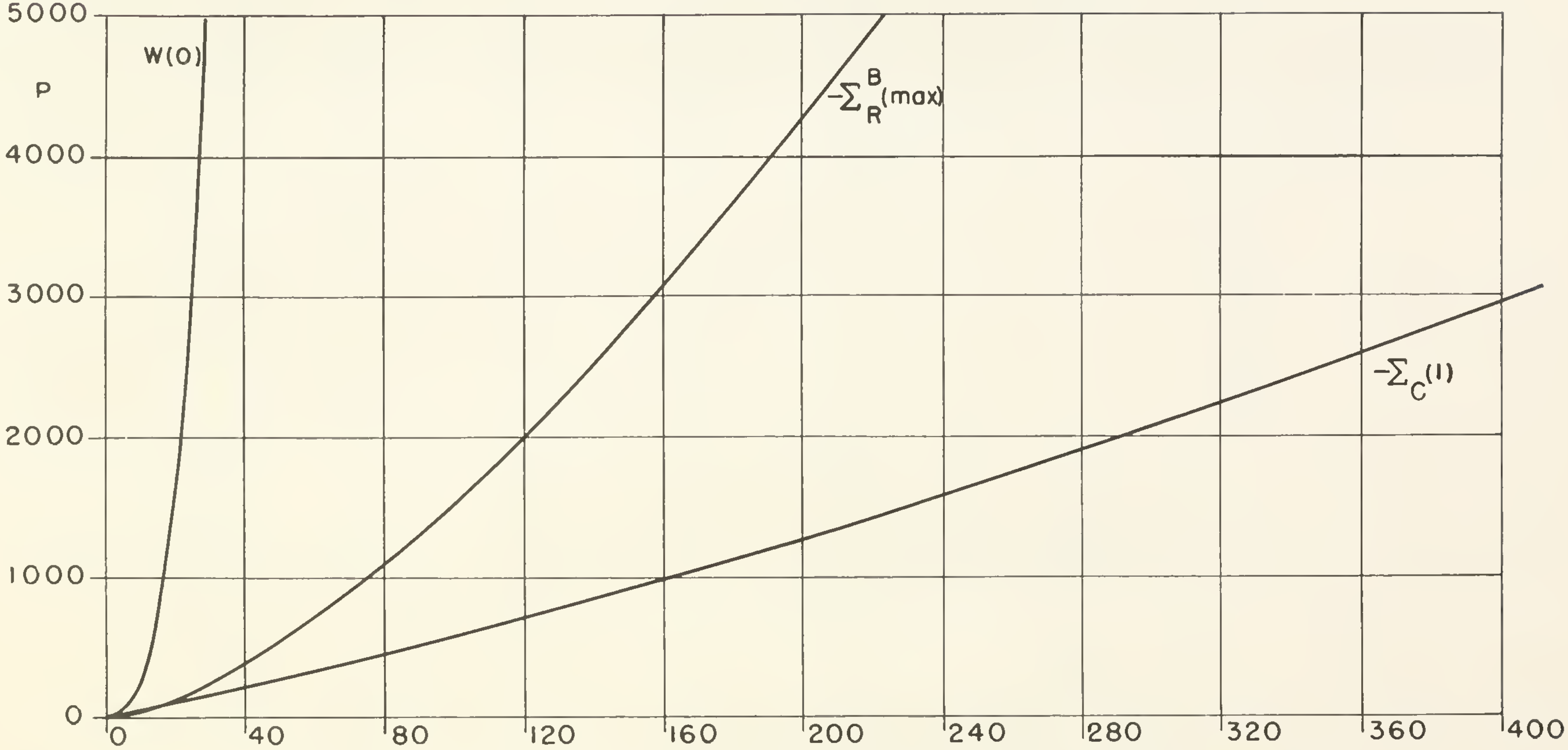
PROBLEM C

Fig. 5c: Maximum Stresses and Deflection at the Center, Problem C.

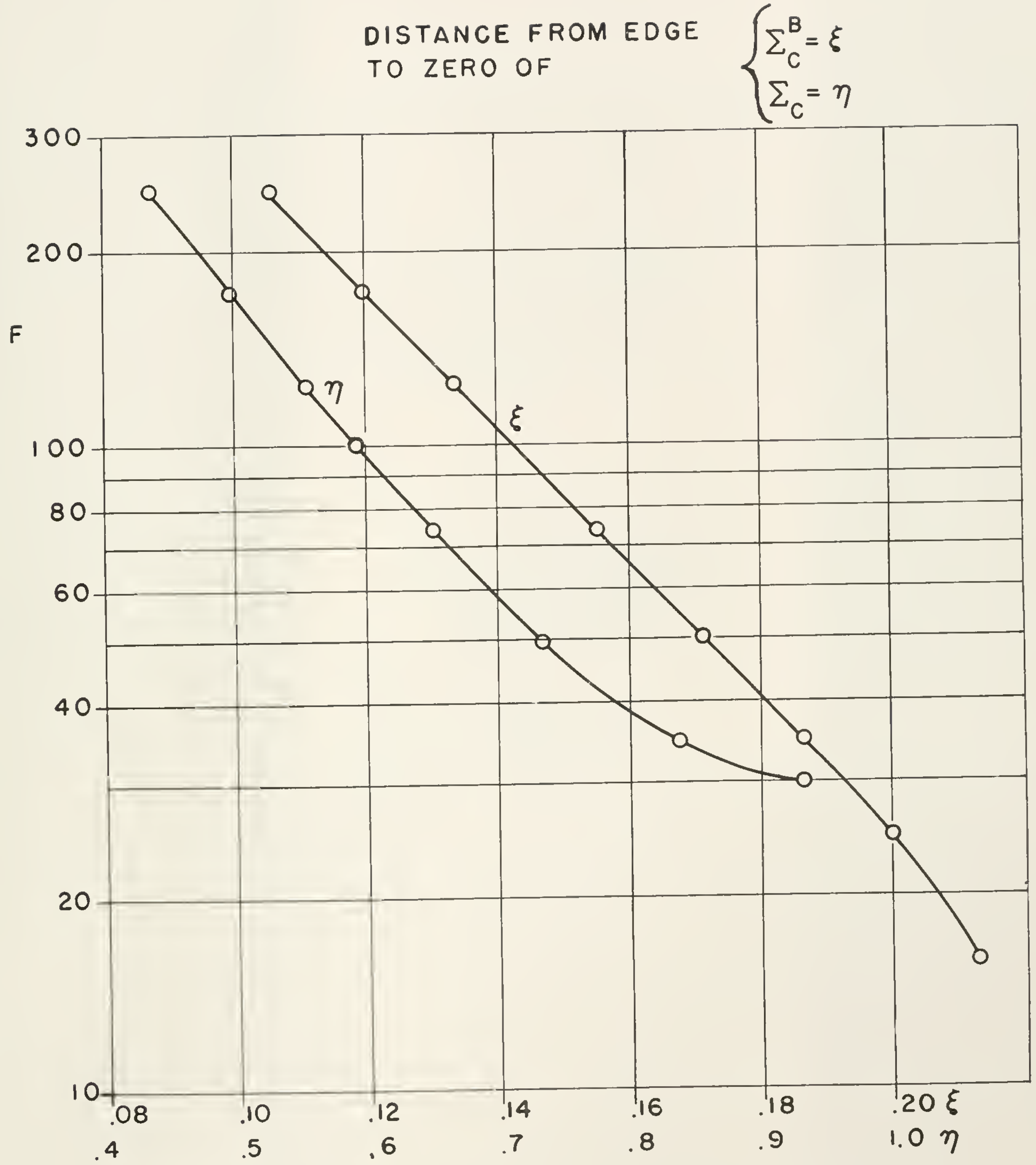

Fig. 6: Variation of Boundary Layer Thickness, Problem E.

C.1

NYO-7978

Keller

NYO-7978

C.1

NYO-7978

C.1

Keller

AUTHOR

Non-Linear Bending and Buckling of Circular Plates. C.1

TITLE

DATE DUE	BORROWER'S NAME	ROOM NUMBER
OCT 16 '62	Murray Schechter	
JAN 4 '63	~~[illegible]~~	
DEC 3 '63	~~[illegible]~~	

N. Y. U. Institute of
Mathematical Sciences
25 Waverly Place
New York 3, N. Y.

MAR 20 1961

Date Due

OCT 16 '62			
JAN 4 '63			
DEC 3 '63			
NOV 7 '66			
SEP 6 '66			

C.1